

Development and Implementation of Real-Time Dynamic Simulation for Gas Turbine Systems in MATLAB/Simulink Environment

Alessandro Bianchi, Luca Fabbri, and Federica Rizzo

Department of Mechanical and Aerospace Engineering, University of Bologna, Italy; Department of Energy, Politecnico di Milano, Italy

Abstract: Dynamic simulation of turbomachinery by Hardware in the Loop (HIL) real-time systems has become an essential practice, due to the high cost of real equipment testing and the need to verify the control and diagnostic systems' reaction to emergency situations. The authors developed a full model of a power generation Gas Turbine Plant, including liquid and gaseous auxiliaries, and the electrical generator and starter motor, integrated in a MATLAB[®]/Simulink[®] simulation suite: *TGSimPlus*[™]. This allows assembling models of various gas turbine (GT) architectures by customised Simulink[®] library blocks and simulating steady state and transient conditions, such as complete start-up and shutdown operations as well as emergency, contingent operations and artificially injected fault scenarios. The model solver runs real-time steps at milliseconds scale. The paper describes the main modelling characteristics and typical results of steady state and transient simulations of a heavy-duty gas turbine under development by Doosan Heavy Industries and Construction (Changwon, South Korea). Comparison with benchmark design simulations obtained by a reference non real-time software shows a good match between the two environments, duly taking into account some differences in the GT models setting affecting parts of the sequence. The paper discusses also the bleed streams warm-up influence on GT performance and the start-up states trajectories dependency on control logic and on the starter helper motor torque envelope.

Keywords: TGSim Plus; real-time simulator; steady state; transient; dynamics; simulation; modelling; gas turbine; MATLAB/Simulink

1. Introduction

1.1. The Need for a Simulator

Dynamic simulation by Hardware in the Loop (HIL) real-time systems has become a common practice in several industrial fields, in particular in the turbomachinery sector, due to the high cost of real equipment testing and the need to verify the control and diagnostic systems reaction to emergency situations or fault conditions that could damage the machinery.

HIL testing consists in interfacing the real prototype or final product control system with a computing platform, which runs a software simulating in real time the dynamic behaviour of the controlled machine or process as if it were the real one in full feedback behaviour, as represented in Figure 1.

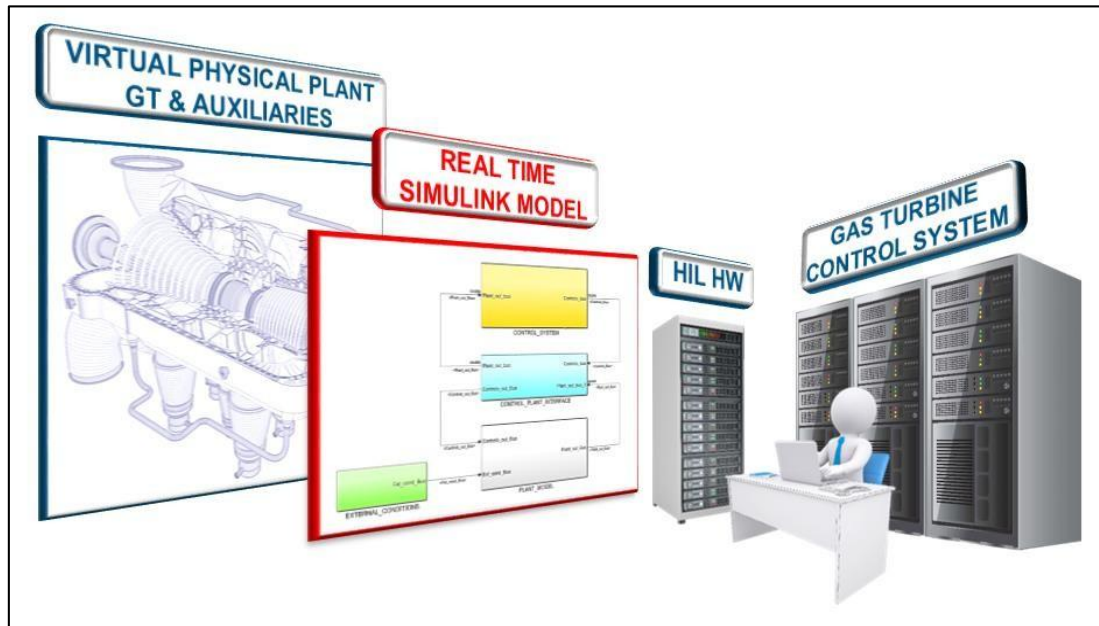


Figure 1. Gas turbine (GT) control system validation and verification by Hardware in the Loop (HIL) testing and simulated physical plant.

In response to this need, the authors developed a full model of a power generation Gas Turbine Plant integrated in a MATLAB®/Simulink® simulation suite, referred to as *TGSim Plus*TM (general information can be found under Supplementary Materials section), which allows simulating steady state and operational transient conditions, as anticipated in previous papers by the authors, reproduced partly here with permission by the publishers [1,2]. This development is based on a twenty-year R&D activity and background in process and rotating machinery modelling and simulation, which included also a simpler version of *TGSim*TM, but based on the same approach. The real-time model can run on any HIL platform compatible with MATLAB®/ Simulink®, although it was tested and delivered for a Multi-Processor HIL platform (MPHILP) by dSPACE GmbH (Paderborn, Germany). The paper illustrates the main features of this model and its base components, such as compressor, combustor and expander, along with typical results of start-up and shutdown simulations. These are compared with data obtained in an actual GT development context by a reference, non-real-time, simulation tool, i.e., NPSS® (Numerical Propulsion System Simulation) by the SWRI (Southwest Research Institute, San Antonio, TX, USA) [3], used by the first licensee of this suite, Doosan Heavy Industries and Construction (DHIC, Changwon, South Korea). DHIC relied on this technology in their development of a large H-class gas turbine, started in 2013 and planned to be completed by 2020. This gas turbine model currently still under development will be supplied to the Gimpo Combined Heat & Power Plant (Gimpo, South Korea), which is run by Korea Western Power (Taeon-eup, South Korea), and is scheduled to start commercial operation in 2023 [4–6]. The comparisons are reported in this article in normalised format, due to confidentiality.

1.2. *TGSim Plus*TM Features

The *TGSim Plus*TM suite was used to model and simulate the whole power generation gas turbine system, including liquid and gas flow auxiliaries, under development by DHIC.

Two types of model were implemented: an online real-time model, to be interfaced with the HIL platform, and an offline standalone model, used for validation with reference data, this latter not necessarily real-time, yet behaving with similar runtime speed.

The gas turbine system model developed includes four main blocks, as represented in Figure 2, each corresponding to a single core of the MPHILP, from top to bottom:

1. Gas Turbine Main Model: gas turbine machine and electric motor–generator system.
2. Gas Turbine Control System (GTCS): real (online model) or simulated version (offline model) of the control system. The former includes the interface with the real control rack through the HIL platform, the other includes the essential controllers and logics in the Simulink® environment needed for the GT and auxiliary systems management in validation or study simulations. The extension of this latter and the level of complexity depends on the level of accuracy and use of the offline model and on the type of validation tests to be performed before starting the HIL tests. In any case the simulated version of the GTCS, used in the offline model, consists of open-loop, feedforward controls and feedback closed-loop controllers, either stand alone or in cascade architectures, depending on the variable to be controlled (i.e., pressures, temperatures, flow rates, liquid levels, shaft speed and GT power controllers). The Simulink® environment and the *TGSim Plus*™ controllers libraries allow a wide and flexible set of solutions that can be fully customized according to the Customer GT specifications or project phase needs. Controllers extend well over the basic PID (proportional–integral–derivative) controllers as any kind of conditional behaviour is implemented in the library blocks, e.g., up/lowclamp, uprate/downrate limits, hold-up/hold-down conditions, etc. The simulated offline version of the GTCS uses discrete-time controllers at the real system sampling time (that is normally longer than the solver sampling time) interfaced with the continuous-time dynamic model of the physical system.
3. Gaseous Auxiliaries Model: auxiliary systems with gaseous fluids, i.e., fuel gas, purge air, cooling, sealing, and compressed air, and GT casing cooling systems.
4. Liquid Auxiliaries Model: auxiliary systems with liquid fluids, i.e., lube and hydraulic oil systems, fuel oil, and water injection systems.

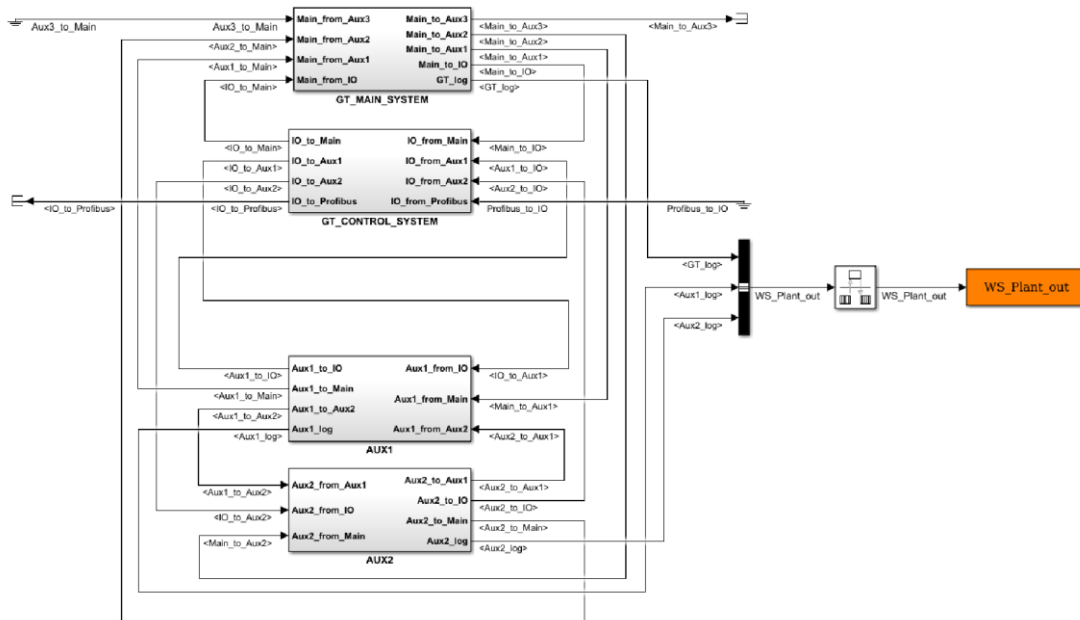


Figure 2. *TGSim Plus*™ main model. Top level architecture.

The thermodynamics of the gas components is based on mapped properties of the base species of air and combustion products, taken from any suitable source, in particular, in the case under study, from the NASA data set and formulation [7]. Other properties of the fluids, e.g., transport properties, are also mapped based mostly on Reid et al. [8].

The mathematical solver is of course set as fixed time step for online simulations, due to the I/O interface and HIL platform characteristics, while for offline simulations, run on stand-alone workstations, it can be either set at fixed or variable time step, according to the various options

available in the Simulink® environment. This allows, particularly during the model development phase, to verify and ensure the limits of the fixed time step vis-à-vis the accuracy obtained.

2. TGSim Plus™ Modelling

2.1. Accumulating and Flow Rate Generating Blocks

TGSimPlus™ is based on 0-D modelling elements, i.e., lumped components [9,10]. Lumped blocks are divided into two major categories: accumulating and flow rate generating blocks.

Accumulating blocks are model blocks which receive as input extensive properties of the fluid, such as mass and enthalpy rates, \dot{m} and $\dot{m}h$ respectively, and give as output intensive properties of the fluid, such as pressure, p , temperature, T , and molar composition, X_m . Examples of accumulating blocks are the gas and liquid flow manifold blocks, where flows mix, and the combustor block, where a chemical reaction also occurs.

Flow rate generating blocks, instead, receive as input intensive properties of the fluid (e.g., p , T , and X_m) and give as output extensive properties of the fluid (e.g., \dot{m}). Flow rate generating blocks include, for instance, the gas and liquid flow restriction and valve blocks, the compressor and the expander blocks, the liquid pump and the cooling air fan blocks.

Accumulating and flow rate generating blocks are always used in topological sequence in the model, thus an accumulating block is always between two flow generating blocks, and vice versa. In the modelling and calculation flow, each block calculates its output based on the feedback received from the subsequent block, while providing in turn its feedback to the preceding block.

2.2. Compressor Modelling

The **TGSimPlus™** compressor block simulates an energy jump on a flowing gas, which depends on:

1. Instantaneous shaft speed,
2. Actual inlet and discharge stream conditions,
3. Inlet guide vane (IGV) angle,
4. Actual performance maps.

The compressor performance maps consist of lookup tables relating:

- the inlet volume flow rate, Q , as function of the shaft speed, N_c , the polytropic head faced by and withstood by the stages set, PH , and IGV angle, or $Q = Q(PH, N_c, IGV)$,
- the polytropic efficiency of the stage set, PE , as function of the shaft speed, the volume flow rate, and the IGV angle, or $PE = PE(Q, N_c, IGV)$.

The polytropic head provided by the compressor stage set, PH , is calculated in (1) according to the instantaneous inlet and discharge stream conditions:

$$PH = \frac{p_2}{p_1} \left(\frac{\rho_1}{\rho_2} \right)^{\frac{1}{n_c}} \quad (1)$$

where n_c is the instantaneous polytropic exponent calculated according to the value of PE , p_1 and p_2 are respectively the inlet and discharge pressure of the stage set, and ρ_1 is the air density at its inlet.

The compressor stage set performance maps are corrected as function of the reference to instantaneous speed of sound ratio, $a_{0,ref}/a_0$, by Equations (2)–(4):

$$a_{0,ref} \quad Q_{corr} = Q \quad (2)$$

$$PH_{corr} = PH \cdot \frac{a_0}{a_0, ref} \quad (3)$$

$$N_{corr} = N_c \cdot \frac{a_0}{a_0, ref} \quad (4)$$

The instantaneous volume flow rate is a dependent quantity, function of the stage set performance map, and is calculated first by interpolation using the table $Q_{corr} = Q_{corr}(PH_{corr}, N_{c,corr}, IGV)$. The polytropic efficiency is then obtained by interpolation using the table $PE = PE(Q_{corr}, N_{c,corr}, IGV)$. The actual flow rate is then obtained by inverting Equation (2). This formulation is a generalization of the customary correction methods [11], to account for gases other than air, and was extensively validated and used for broad sets of dynamic compressors and expanders [12–14].

The **TGSim Plus**TM compressor library includes two categories of blocks: the *single-map* and the *multiple-map* compressor blocks, represented schematically in Figure 3.

The *single-map* compressor block (SMC), Figure 3a, yields the mass flow rate generated by the compressor and entering its inlet side (gross of bleed extraction flow rates) according to the total head, between discharge and inlet sections, based on a single map, representing the whole machine stage set. The *multiple-map* compressor block (MMC) consists of several (e.g., three) compressor blocks, Figure 3b. From the topology point of view, these are similar to a SMC block, each with different maps calculating the respective dependent quantities from the boundary ones. The three stage sets included in the example MMC block are separated by two lumped volumes, where mass and energy balances account for gas and thermal accumulation, thus delayed pressure changes in transients. This distributed accumulation and delay cannot be simulated by the SMC model, since it considers the compressor as a whole. In the MMC model the whole head is dynamically split among the stages sets, depending on the balances in the intermediate volumes and on the bleed flow dynamics.

The SMC and MMC blocks differ also for what regards the bleed management. In the SMC model, the bleed pressure and temperature are calculated according to the instantaneous partial enthalpy jump associated to the bleed stage, as fraction of the whole one. The bleed mass flow rates are calculated according to the pressure difference between the compressor bleed port and the downstream volume, along the bleed line.

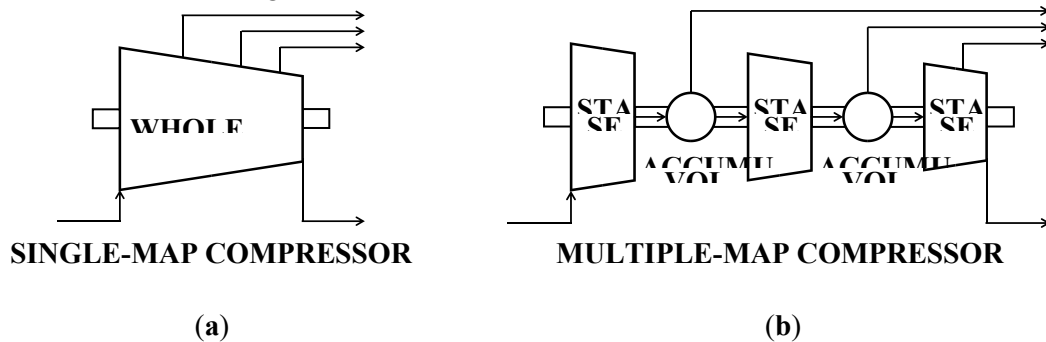


Figure 3. **TGSimPlus**TMcompressormodelling. (a)Single-mapcompressor, (b)Multiple-mapcompressor.

In the MMC model, instead, the bleed pressure and temperature, for the first and the second bleed stages of Figure 3b, result dynamically from the mass and energy balances in the intermediate lumped volumes. In this case, the bleed mass flow rates are calculated according to the pressure difference between the corresponding intermediate volume, and the downstream volume along the bleed line.

The last bleed stage, in the example MMC of Figure 3b, is extracted from within the rear compressor block. This is then treated like an SMC bleed port and flow.

The SMC and MMC blocks allow adapting the compressor modelling based on the maps available at the stage of development of the model, e.g., initially by an SMC and later, when more detailed maps are available, by MMC.

2.3. Combustor Modelling

In *TGSim Plus*TM the combustor model is a two-zone one, in which the transformations occurring in the combustion process are assumed to be divided into the following subsequent processes:

1. Stoichiometric combustion of fuel, gas or liquid or both, with dry air, assumed adiabatic and isobaric.
2. Mixing process of the stoichiometric combustion products with the inert air and water vapour, occurring in a lumped volume, where the mass and energy balances account for the thermal exchange with the burner walls and determine the combustion pressure.

Figure 4 illustrates the main flows and calculation processes considered in *TGSim Plus*TM combustor block, i.e., streams pre-mixing, streams separation, stoichiometric combustion, and mixing.

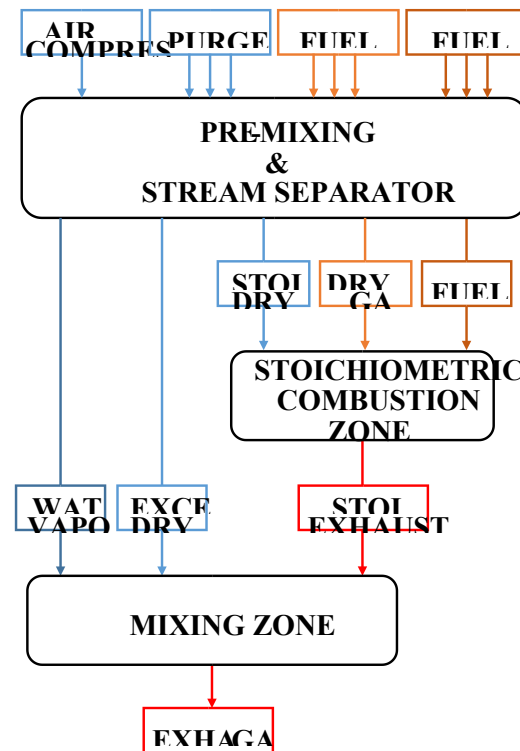


Figure 4. Schematic of the internal structure of *TGSim Plus*TM combustor block.

In the streams pre-mixing process, all the gas and liquid flows coming from the separate lines of the plant, i.e., from compressor, purge air, fuel gas and fuel oil system, are merged to form two different streams: gaseous fuel gas and air mixture, and liquid fuel oil.

The gaseous flow stream passes then through a stream separator, which rearranges the different species into three streams: the fuel gas and air components are separated from the mixture and split into dry fuel gas, dry air and water vapour streams. The dry air flow is further divided into two streams: the stoichiometric part, taken to react with either dry fuel streams, going to the stoichiometric combustion zone, and the excess air, going to the mixing zone. The three streams of stoichiometric dry air, dry fuel gas, and fuel oil react in the stoichiometric combustion zone, yielding the stoichiometric exhaust gas stream.

The fuel gas combustion, in the current implementation of *TGSim Plus*TM combustor, considers the reaction of arbitrary mixtures of ideal gases made up of the following gas species given as molar fraction data: Argon, Carbon dioxide, Nitrogen, Oxygen, Water vapour, Methane, Ethane, Propane, n-Butane, i-Butane.

The combustion process of fuel oil, instead, is based on the atomic hydrogen/carbon ratio (H/C) given as average liquid fuel datum. The stoichiometric products are then mixed with the water vapour previously extracted and the excess dry air, which do not take part to the stoichiometric combustion, resulting into the hot exhaust gas flowing out toward the expander.

The *TGSim Plus*TM combustor block can operate with dual fuel and manages the presence of flame based on a logic which takes into account four logical conditions, namely:

1. Fuel mass flow rate, checking the actual presence of fuel flow in the combustor.
2. Air mass flow rate, checking the actual presence of air flow in the combustor.
3. Stoichiometric air mass flow rate, checking that the stoichiometric air flow required to burn the whole fuel flow is lower than the air flow rate from the compressor, i.e., that the air flow is sufficient to burn all the fuel being injected in the combustion chamber.
4. Ignition command, checking that the ignition command signal is ON.

Only when all the above conditions are satisfied the combustion process is enabled. Should the combustion process be disabled, no stoichiometric exhaust gas is generated and the streams of stoichiometric dry air and unburnt dry fuel are directly passed to the mixing zone, where they mix again with the streams of excess dry air and water vapour. When fuel oil is used, if the combustion is disabled but fuel oil was injected anyway by the control system by any reason, the combustor block yields a stream of unburnt fuel oil.

2.4. Expander Modelling

Similarly to the case of the compressor block, the *TGSim Plus*TM expander block simulates an energy jump on a flowing gas, which depends on:

1. Instantaneous shaft speed,
2. Actual inlet and discharge stream conditions,
3. Actual performance maps.

The expander performance maps usually consist of lookup tables of corrected mass flow rate, \dot{m}' , and isentropic efficiency, $\eta_{t,is}$, as functions of the expander shaft speed, N_t , and the expansion ratio, π_t , i.e., $\dot{m}' = \dot{m}'(N_t, \pi_t)$ and $\eta_{t,is} = \eta_{t,is}(N_t, \pi_t)$.

The isentropic enthalpy jump produced by the expander, Δh_{is} , is calculated in (5) according to the actual inlet and discharge stream conditions:

$$\Delta h_{is} = h_3 - h_{4is} \quad (5)$$

where h_3 is the enthalpy at the expander inlet and h_{4is} is the enthalpy that would be obtained at the expander outlet by an isentropic expansion, obtained from the gas composition and the discharge isentropic temperature, T_{4is} , which is itself function of the inlet pressure and temperature, the discharge pressure, and the gas composition, i.e., $T_{4is} = T_{4is}(p_3, T_3, p_4, X_m)$, through the relative pressure function of the mixture.

The instantaneous mass flow rate is function of the expander performance map, i.e., it is calculated by interpolating the table $\dot{m}' = \dot{m}'(N_t, \pi_t)$. The isentropic efficiency is also obtained by interpolating the table $\eta_{t,is} = \eta_{t,is}(N_t, \pi_t)$, yielding finally the actual outlet enthalpy.

The expander performance maps are corrected as function of the ratios between the reference values of speed of sound, pressure, and heat capacity ratio, $a_{0,ref}$, p_{ref} , and γ_{ref} , and their actual values at the expander inlet, a_0 , p , and γ , by Equations (6) and (7):

$$m_c = m_{pref} \frac{a_{0,ref}}{a_0} \frac{\gamma_{ref}}{\gamma} \frac{p}{p_{ref}} \quad (6)_{corr}$$

$$N_{tcorr} = N_t \frac{a_{0,ref}}{a_0} \quad (7)$$

Given the usually low number of expansion stages, the **TGSimPlus™** expander block is modelled as a single-map expander, managing a single map which is representative of the performance of the whole expander. The multi-map modelling option would be possible like for the compressor, should the map data be available for separate stages or groups thereof, but at the expense of calculation time.

In the **TGSim Plus™** expander block the cooling streams extracted from the compressor are accurately modelled to better match test data. The cooling pressure at the intermediate stages, p_b , is calculated in Equation (8) from the expander inlet pressure according to the stage number of the cooling bleed port:

$$p_4 = p_3 \left(\frac{p_b}{p_3} \right)^{\frac{n_{st}}{n_{st,tot}}} \quad (8)$$

where p_3 and p_4 are respectively the expander inlet and discharge pressures, and n_{st} and $n_{st,tot}$ are respectively the expander cooling bleed port stage and the total number of stages of the expander.

To account for the cooling streams warm-up due to heat leakages from equipment mass along the bleed lines from compressor to expander, their temperature is calculated by Equation (9):

$$T_b = T_{b,c} + k_h (T_{b,t} - T_{b,c}) \quad (9)$$

where k_h is a dimensionless tunable parameter, which can vary in the range [0,1], $T_{b,c}$ is the temperature at the bleed port calculated by the compressor block, $T_{b,t}$ is the temperature of the inlet stream at the expander cooling bleed port, calculated in Equation (10) as function of the expander inlet pressure and temperature, p_3 and T_3 , the expansion polytropic exponent, n_t , and the cooling pressure at the intermediate stage, p_b , obtained from Equation (8):

$$T_{b,t} = T_3 \left(\frac{p_b}{p_3} \right)^{\frac{n_t-1}{n_t}} \quad (10)$$

The corresponding heat leakage power is subtracted by the cooling bleed flows from the main inlet lumped volume, and its wall mass, before entering the expander.

The cooling bleed flows contribute to the machine power, by expanding down to the expander discharge pressure. The isentropic efficiency for their expansion, $\eta_{b,t,is}$, is assumed equal to that calculated by the maps for the expander main flow, $\eta_{t,is}$, i.e., $\eta_{b,t,is} = \eta_{t,is}(N_b, \pi_t)$, which is an acceptable approximation.

The results of a power-controlled steady-state sensitivity analysis varying the value of k_h through the full range [0,1] at full-speed full-load conditions (FSFL) are presented in normalised form in Figure 5.

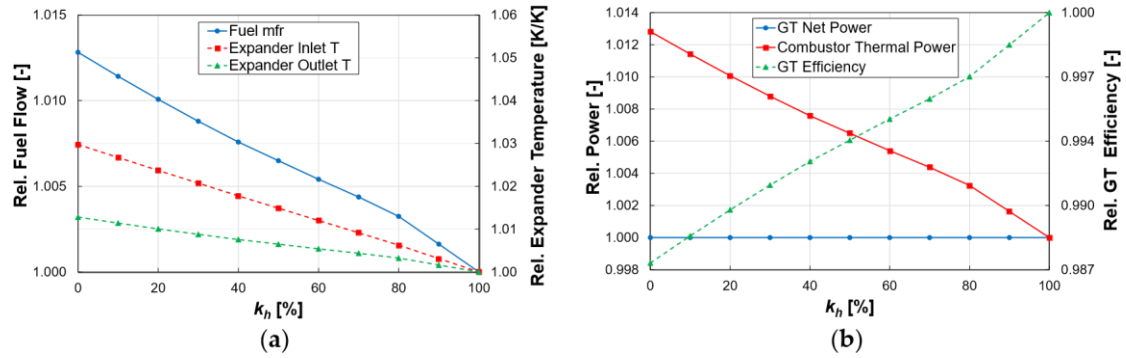


Figure 5. *TGSimPlus*[™] results of a steady state sensitivity analysis varying the value of k_h . The results are normalised with respect to the corresponding values at $k_h = 1$. (a) Primary axis: normalised fuel gas mass flow rate (solid blue line); Secondary axis: normalised expander inlet and outlet temperatures (dashed red and green lines respectively), (b) Primary axis: normalised GT net power and combustion thermal power (solid blue and red lines respectively); Secondary axis: normalised GT efficiency (dashed green line).

These plots are consistent with the expected behaviour. Indeed the net power is constant because the conditions simulated are under constant power set point to the control system, which acts on the fuel rate. This therefore varies to follow the change in the GT cycle efficiency, which is lower when the bleed flows enter their expansion ports at low temperature (low k_h). The user can improve the fidelity of the model, by adjusting this parameter when detailed design or previous data on existing GTs or experimental data are available for the GT being simulated by HIL tests.

2.5. Electric Motor and Generator

TGSim Plus[™] includes the modelling of an electrical system and machine, referred to as Electric Starter Motor (EM) and Electrical Synchronous Generator (EG). The Electric Motor and Generator (EMG) block can operate in two mutually exclusive functional modes, activated as function of the GT operational phase: the *EM mode*, involving the Static Frequency Converter (SFC) and its internal control, driving the variable-speed electric motor, which simulates the starter helper motor; the *EG mode*, involving the model of a synchronous type electrical generator, which simulates the load applied to the GT system before and after the connection to grid.

The EMG block calculates the instantaneous value of the mechanical torque applied to the GT driveline shaft and the dynamic balance of the GT driveline, considering the net GT torque (including the bearings friction), the EMG torque, and the GT and EMG rotational inertia.

Each mode provides the instantaneous value of the mechanical torque applied to the GT driveline shaft, $T_{q,EMG}$, calculated according to its instantaneous conditions. The EMG block includes also the dynamic balance of the GT driveline, expressed by Equation (11):

$$\frac{d\omega}{dt} = \frac{1}{J_{dr}} (T_{q,dr} - T_{q,EMG}) \quad (11)$$

where $d\omega/dt$ is the angular speed derivative, function of the resultant torque, defined as the algebraic sum of the net GT torque, $T_{q,dr}$, of the EMG torque, $T_{q,EMG}$, and of the GT and EMG inertia, J_{dr} . The net GT torque is given by the expander torque less the compressor torque and the bearings friction.

The EM-SFC system is simulated as a variable-torque generator based on a closed loop EM speed controller that generates an instantaneous active torque, which may be lower than or equal to the limit provided by its maximum torque-speed envelope function, according to the speed set point and the feedback error. This closed loop controller simulates the dynamics of internal current and frequency controllers of the SFC and EM as an equivalent dynamic block and allows simulating all

the speed control functionalities and logics and the enabling and disabling commands of the EM mode. In this latter mode the (positive) torque applied to the driveline rotational balance is added to the net GT torque, which can be positive or negative as function of the speed and the status of combustor, IGV angle and bleed valves. The SFC controller minimum output is a null value, which means that the driveline can coast down only by the compressor load and bearing friction.

When the GT speed controller is enabled and the EG is disconnected from the grid, the net GT power must balance the inertia of the driveline according to the acceleration required. In this condition the shaft balance provides the instantaneous angular speed, which can vary ramping-up to the synchronization speed and then oscillating around the latter until entering a given threshold tolerance for connection. Once the EG is connected to the grid, the driveline speed becomes an exogenous input to the system, either constant or disturbed like in real power GT operation. In this condition the GT is turned to closed loop power control.

3. Typical Results

3.1. Comparison Start-Up Simulation, from Purge Speed to FSFL and Shut Down

Typical results of a transient simulation from start-up to power and to shutdown using *TGSim Plus*TM are shown in Figure 6 comparing the reference data obtained by a design tool [3] and the output provided by *TGSim Plus*TM. The results are reported in normalised form with respect to the values of the respective variable at FSFL in the component considered. Temperatures are normalised as absolute values ratios [K/K].

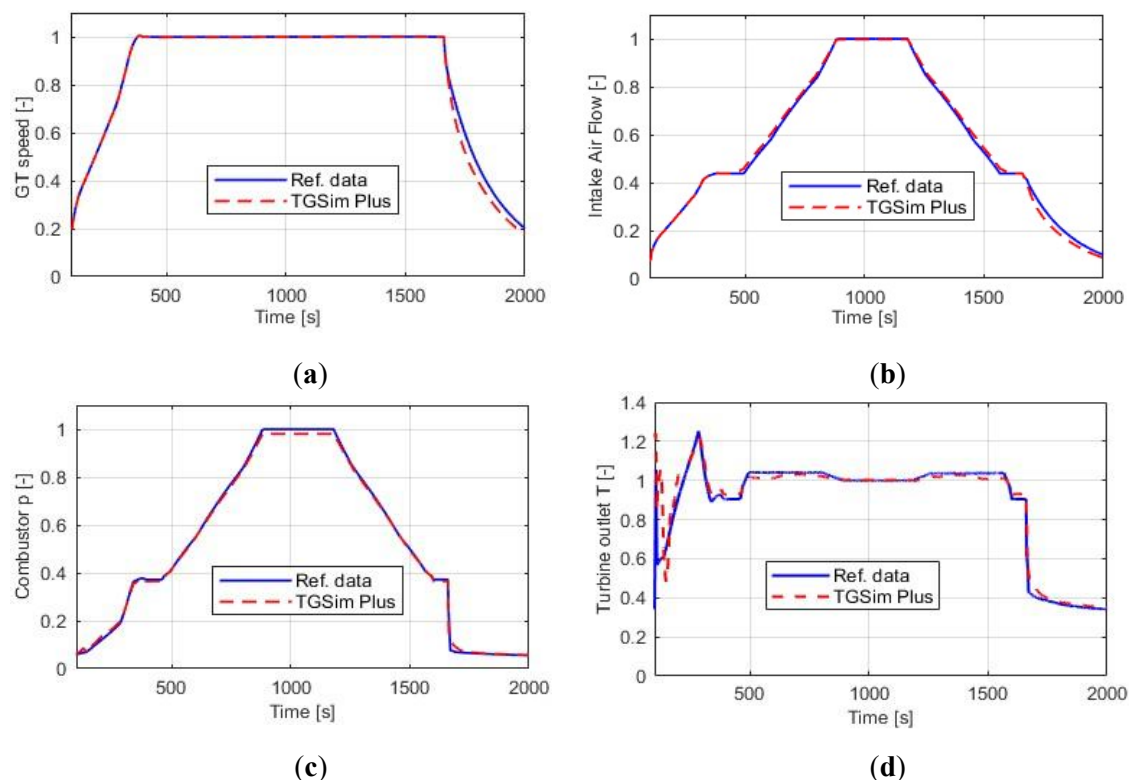


Figure 6. Results of start-up and shutdown simulation. Comparison between reference data (solid blue line) and *TGSim Plus*TM results (dashed red line). (a) Normalised rotational speed, (b) Normalised compressor intake mass flow rate, (c) Normalised combustor discharge pressure, (d) Normalised expander discharge temperature.

The gas turbine system is simulated from the ignition speed up to full-speed no-load conditions

(FSNL), then from FSNL to FSFL, reaching steady state conditions. The load was then reduced back to FSNL condition, which is finally followed by the shutdown phase.

In order to allow comparing reference data with *TGSim Plus*TM results obtained by an offline simulation, this latter was performed using as exogenous input to the model the reference signals for speed (as set point), load power, and IGV angle. The gas turbine operates under speed control for the whole simulation, subject to all other dynamics: thermal, fluid-dynamic, rotational and other controllers'.

The plots of Figure 6 show that *TGSim Plus*TM matches quite well the reference data, both during the transient phases and the steady state conditions. The percent deviations at FSFL are reported in Table 1 for compressor intake mass flow rate, combustor discharge temperature, combustor discharge pressure, and expander discharge temperature.

Table 1. Percent deviations between reference data and *TGSim Plus*TM results at Full-Speed Full-Load (FSFL). Note that temperature deviations are based on a normalisation on temperature values in [K].

| Description | Deviation |
|----------------------------------|-----------|
| Compressor intake mass flow rate | -0.28% |
| Combustor discharge temperature | -1.13% |
| Combustor discharge pressure | -1.96% |
| Expander discharge temperature | +0.20% |

3.2. Analysis of the GT Start-Up, from Rest to FSNL

This section shows and discusses a more detailed sequence of the start-up of the GT system, simulated by *TGSim Plus*TM in offline mode as part of an internal R&D study by the authors, independent from the DHIC project. The complete start-up sequence is defined by the following broad steps, from rest to power condition:

- Start and warm-up phase at low speed (20% of nominal), from 0 s to 1200 s, in EM-SFC mode under speed control, switching on fuel gas between 1000 s and 1200 s;
- Initial ramp-up phase, from 1200 s to 1300 s, driven both by the EM-SFC and by the GT under fuel gas speed controller, acting concurrently up to the EM-SFC switch-off speed;
- Final ramp-up phase to Full-Speed No-Load conditions (FSNL), in continuity with the former, from 1300 s to 1600 s, driven only by the GT under fuel gas speed controller;
- Synchronization and connection to grid and power increase up to Full-Speed Full-Load (FSFL) or a partial demanded load in EG mode by the fuel gas power controller.

The results reported herewith focus on the first three steps. A first setup, referred to as Case 0, was analysed in the frameworks of a design phase of the GT system and verification of its operations and control system and logic tuning. Two additional simulations were taken into account, respectively Case 1 and Case 2, representing alternatives to obtain an improved and more efficient start-up sequence.

As shown in Figure 7 and in the left-side plot of Figure 8, the start-up sequence implemented as per Case 0 would be affected by excessive temperature peaks in the combustion chamber and flow instabilities due to compressor surge during step c). These problems derive from a common root cause: indeed, the high acceleration demand imposed to the GT system, which is generally justified by the need of bringing power generation GTs to operation quickly (e.g., within 300 s), goes with lack of torque in part of the ramp-up phase.

Soon after start of ramping up, the SFC-EM torque is brought to its maximum value compatible with its power limit, which implies a torque decaying trend, inversely proportional to speed (Figure 9). The total driving torque, i.e., the sum of the EM-SFC and of the GT ones, becomes insufficient to

follow the speed set point, at about half of the nominal speed. The GT speed controller, therefore, demands greater fuel rate to compensate the lack of speed. On one side, this causes a pressure increase in the combustion chamber that produces an increase of the expander torque but also an increase of the pressure ratio and head faced by the compressor, with consequent upwards move of its operating point across the performance map. Since its passive torque increases too, the net driver torque becomes even more insufficient, causing a temporary speed saturation and slight reduction, while the compressor operating point moves leftwards, beyond the surge line. This causes air flow instability and a temporary ceiling of the average flow rate delivered by the compressor, as also reported in the literature [15].

Meanwhile, the increased fuel rate, not accompanied by a higher air flow, determines an increase of the combustion temperature, which exceeds the design threshold.

As a remedy to the lack of torque, two alternatives were analysed:

- (1) reducing the acceleration demand (Case 1), or
- (2) increasing the power rating of the EM-SFC (Case 2).

Table 2 summarises the main simulations results, reporting the comparison of the ramp-up time required to reach FSNL, from the warm-up speed, the maximum normalised acceleration, the maximum normalised temperature reached in the combustor and the time lapsed beyond its limit.

- In Case 0 the acceleration ramp from ignition speed to synchronization speed is performed quite fast, but is characterised by a high acceleration peak along with excessive temperatures in the combustion chamber.
- In Case 1, by implementing a lower slope acceleration ramp, the full speed is reached in a longer time, with a lower acceleration peak and acceptable temperature values in the combustor.
- In Case 2, with a higher SFC torque limit, the GT system maintains the acceleration ramp of Case 0, but with lower acceleration and temperature peaks with respect to both Case 0 and Case 1.

Table 2. Start-up simulations to full-speed no-load (FSNL)—Comparison of features.

| Simulation | Ramp-Up Time | Max. Acceleration | Max. Temperature | C.C. Temperature Exceedance Duration |
|------------|----------------|-------------------|------------------|--------------------------------------|
| | t_{ramp} [s] | $dN\%/dt$ [%/s] | TCC_{max} [–] | Δt_{exc} [s] |
| CASE 0 | | 0.69 | 1.297 | |
| CASE 1 | | 0.52 | 1.041 | |
| CASE 2 | | 0.50 | 1.037 | |

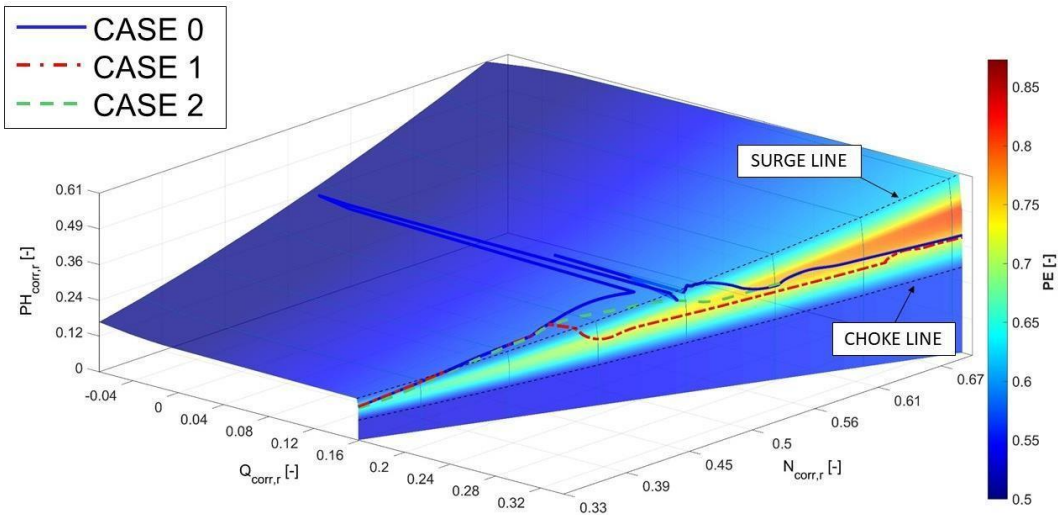


Figure 7. Start-up simulation up to Grid Synchronization. Compressor operative point on the performance map corrected with respect to the speed of sound and expressed in terms of volume flow rate, polytropic head, speed, and polytropic efficiency. All these variables are normalized with respect to their FSFL values.

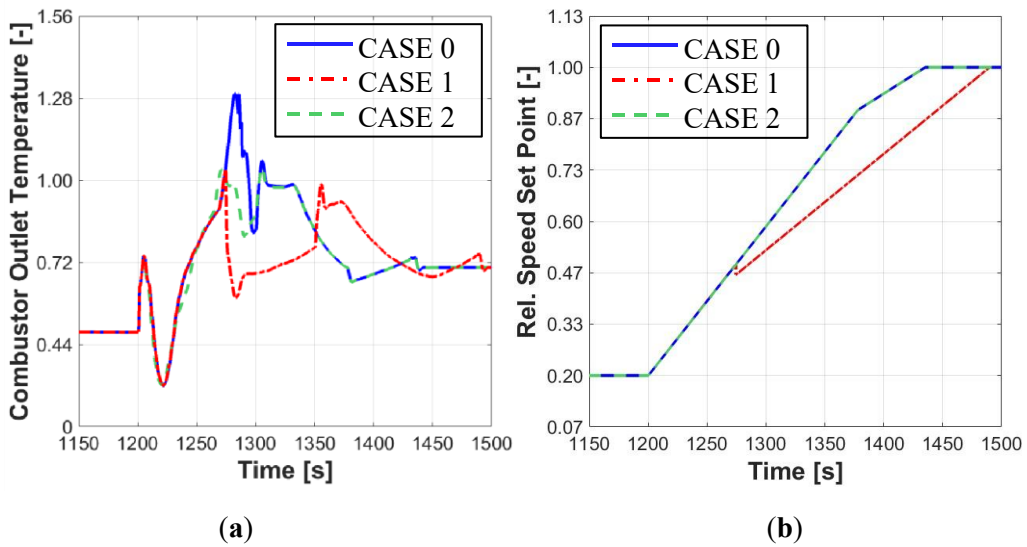
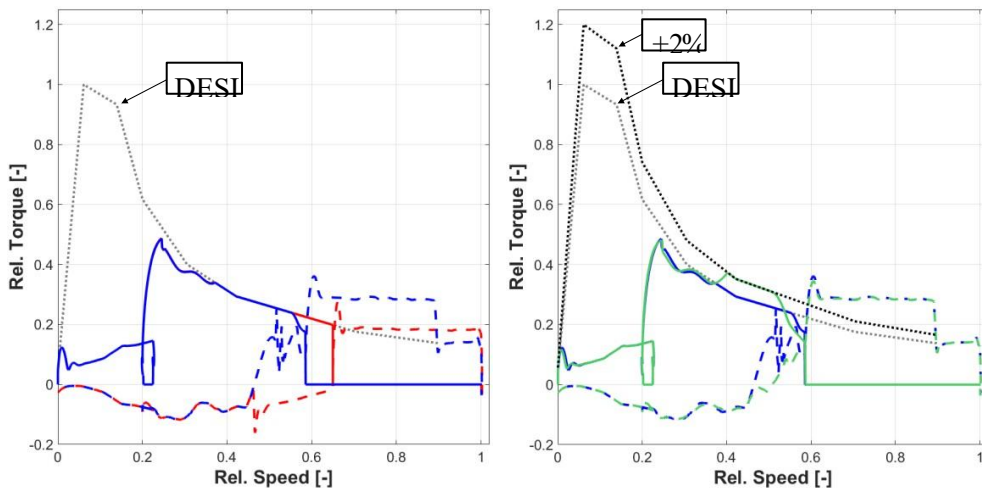


Figure 8. Start-up simulation up to Grid Synchronization. Left: Combustor temperature normalised with respect to the maximum temperature allowed. Right: Normalised speed set point.



| COLOUR | STYLE | |
|----------|-------|----------------|
| ● CASE 0 | — | EMG TORQUE |
| ● CASE 1 | - - - | GT TORQUE |
| ● CASE 2 | | SFC MAX TORQUE |

Figure 9. Start-up simulation up to Grid Synchronization. Normalised Static Frequency Converter (SFC) maximum torque curve, Electric Motor and Generator (EMG) and GT torques varying the normalised speed.

4. Discussion

4.1. Comparison Start-Up Simulation, from Purge Speed to FSFL and Shut Down

The main differences between the reference data and *TGSim Plus*TM results reported in Section 3.1 occur in the transient phases, during shutdown for the rotational speed and the compressor intake flow, as in Figure 6a,b, and both during start-up and shutdown for the combustor discharge temperature and the expander discharge temperature, with minor percent deviations during the loading and unloading phases, as shown in Figure 6d.

The different behaviour during the early start-up phase is due to a mismatch of the fuel rate between the reference and the *TGSim Plus*TM simulations due to the totally different management of the start-up motor in the two cases, which could not be matched completely, in lack of details about the reference one. After the start-up motor shutdown the GT speed controller, acting on the fuel rate, takes full and comparable control, thus the differences in the combustor and expander outlet temperatures become much lower.

The different behaviour during the GT shutdown phase is caused by the different flows in the cooling and bleed lines in the reference and *TGSim Plus*TM simulations. These differences are due to the cooling and bleed control actions and to different estimates of the relative lines' flow coefficients. These different flows have an obvious impact on the various volumes balances thus on the trend of some variables. In support of this argument, it was shown that by rearranging the pressure loss parameters among the cooling and bleed piping and some control logics, the simulated behaviour would better match the reference one, confirming the importance of these data and of their control system tuning.

4.2. Analysis of the GT Start-Up, from Rest to FSNL

The deeper sensitivity analysis made on the early start-up phases of the sequence described in Section 3.2, showed how different can this part of the transients result, depending on the logics adopted and on the interaction among the several phenomena and subsystems.

As shown on the right-side plot of Figure 8, in the ramp-up phase the speed set point follows two linear ramps, with a lower acceleration on approaching the nominal speed. In Case 1 the acceleration demand is reduced in the critical speed range found, as the high-acceleration ramp is maintained for a shorter duration along the lower speed range, thus the speed set point crosses that range by a reduced slope compared to the base Case 0 and Case 2.

Figure 9 shows the torque-speed trajectory of the EMG and of the GT from rest to the synchronization speed, displaying also the maximum torque available by the EM-SFC. It is apparent that in both Cases 0 and 1 the EM-SFC torque saturates dynamically to the limit.

In Case 0, the EM-SFC torque is then insufficient, vis à vis the total torque demand and that available by the GT, yielding the observed higher fuel gas rate and consequent unacceptable temperature in the combustion chamber.

In Case 1, instead, even if saturated, the EM-SFC torque–speed characteristic allows meeting the acceleration set point, lower than in Case 0, yet at the expense of the ramp-up time. In this case, the EM-SFC operation lasts longer, by 50 s, than in the other cases, to exploit its contribution at best.

In Case 2, on its own, it is investigated whether the same acceleration ramp of Case 0 can be met by overrating the EM-SFC by 20%, with respect to the base design. Under this hypothesis, the EM-SFC torque saturates dynamically to its new limit curve for a shorter period and, even if it cannot supply, alone, the torque requested by the acceleration set point up to its switch-off, thus requiring a torque contribution also by the GT and a gradual increase of the fuel gas flow rate, neither compressor surge nor excessive temperatures in the combustor do occur, since the GT operating envelope is always compatible with the torque demand along all the speed ramp.

In both Cases 1 and 2, due to the wider margin between the torque required and that available during the crossing of the critical speed range up to the EM-SFC switch-off, the compressor operating point exceeds slightly the surge line but without entering instability regions. In both of these cases, therefore, the compressor surge is avoided but, above all, the temperature peaks in the combustion chamber do not exceed the design threshold (i.e., the value of 1 in Figure 8) or just do for a very short time.

4.3. Comparison with Other Commercial Software

TGSimPlus™ is a dynamic simulation tool specifically conceived to simulate gas turbine systems, based on tailoring the Simulink® environment and previous libraries developed by SATE for this domain. Indeed, SATE developed the first simulator of this kind in 1999, but later it expanded the set of general purpose libraries for thermodynamic systems keeping pace also with the evolution of the Simulink® environment since. Simulink® was selected as the developed environment as it is a de facto standard in the dynamic simulation community, yet not the unique [16], suitable for control systems analysis, parameters identification and optimization, automatic code generation for real-time and HIL tests simulations.

Other tools exist that might be used for gas turbine process modelling (e.g., HYSYS® by Aspen Technology, Easy5™ by MSC Software, 3KEYMASTER™ by WSC, etc.), but not all of them are suited to real-time and HIL simulations or handling fast dynamics, like shutdown or trip transients.

TGSim Plus™ is based both on general purpose application library blocks, based on 0-D lumped elements, such as volumes, restrictions, valves and heat exchanger segments, both for compressible and incompressible flow conditions, and specific libraries for gas turbine elements, such as single and multistage compressors with intermediate bleed ports, multi-fuel combustion chambers and turboexpanders with cooling inlet flow ports, as discussed above. The majority of the commercial tools includes only low level building blocks, e.g., thermodynamic, fluid dynamic and electrical-mechanical ones, which are not ready-to-use gas turbine components, with the needed flexibility and specialised pre-processing interfaces that **TGSim Plus™** features. Users of those commercial tools have then to build their own gas turbine specific blocks, similarly to what SATE did by tailoring to this application Simulink® and its previous gas systems modelling products (i.e., COMPSYS™, COMPSYS MCwI™,

TGSim™). Therefore, even if relying on a library based approach, similarly to many other tools, **TGSim Plus™** is provided with libraries specific for gas turbine systems.

Moreover, **TGSim Plus™** is based on Simulink® subsystems interconnections, made of buses or standalone signals, which represent *functional* interconnections and not only *physical* interfaces. This interconnection approach has both pros and cons: connecting blocks with **TGSim Plus™** requires indeed more awareness by the user of the physical and control feedbacks in the system, but gives an easier and more evident access to each physical quantity (based on standardised streams and I/O buses) and to the controlled variables of relevance for the control system interfacing, whether by the real one through the HIL interface or by its offline simulated version. Users familiar with the

Simulink® environment will find this representation more convenient as it is common to any kind of dynamic model. The level of training in either cases depends on the user starting background.

Regarding the real-time compatibility, other environments, such as Easy5™ and 3KEYMASTER™, are claimed for real-time simulations. However, it is unknown to the authors whether the sampling time of the simulation solver of these tools can be small enough to be compatible with the needs of HIL tests. Indeed in these applications the signals interface rate with the GTCS must be lower enough than the real controllers', i.e., at millisecond scale on one side, to avoid instabilities, but long enough as to feature a calculation turnaround time (that depends on the HIL platform capability and model complexity) lower than the solver and signals interface time step. It must be highlighted that usually thermal process dynamics, for which most of the cited simulation tools were developed, are slower than the machine ones, which makes a fundamental difference in the performances and accuracy of real-time simulators.

5. Conclusions

The R&D and software implementation work summarised in this paper brought to a powerful tool for the simulation of complete GT systems, i.e., *TGSimPlus*™. This tool can be used both in offline mode, during the GT design phase to optimise and check the control strategies, relying on built-in control functions and library blocks, as well as in real-time online mode for the actual control system verification and tests prior to its coupling with the real machinery.

Despite some differences between the reference data and *TGSim Plus*™ in the validation tests in transient simulations, which were explained in Sections 3.1 and 4.1, these fell within the accuracy requirements set forth by the first licensee, DHIC, which approved the tests performed and the much wider functionalities and real-time behaviour of the simulator.

The more detailed simulation sequences discussed in Sections 3.2 and 4.2 as part of the R&D work performed by the authors, show that *TGSim Plus*™ is suitable also for detailed offline analyses and study simulation to help turbomachinery designers and plant engineers in the investigation of the dynamic behaviour of GT systems and in the definition of efficient operation sequences.

References

1. Brighenti, A.; Duranti, D.; Quintabà, D. *Dynamic Simulation*; Hydrocarbon Engineering, Palladian Publications: Farnham, Surrey, UK, 2019; Volume 24, pp. 65–68. Available online: <https://www.hydrocarbonengineering.com/> (accessed on 2 June 2020).
2. Brighenti, A.; Duranti, D.; Quintabà, D. Real-Time simulation of Gas Turbine systems. In Proceedings of the 35th International CAE Conference, Vicenza, Italy, 28–29 October 2019; Available online: <http://meeting2019.enginsoft.it/> (accessed on 25 June 2019).
3. Numerical Propulsion System Simulation (NPSS). Available online: <https://www.swri.org/consortia/numerical-propulsion-system-simulation-npss> (accessed on 25 June 2019).
4. Power Plant Equipment—Gas Turbines. Available online: <http://www.doosanheavy.com/en/products/energy/tools/> (accessed on 2 June 2020).
5. Doosan Heavy Industries Deploying First Large-Class Gas Turbine for Korean Demonstration Project. Available online: <https://www.power-eng.com/2020/01/03/doosan-heavy-industries-deploying-first-largeclass-gas-turbine-for-korean-demonstration-project/#gref> (accessed on 2 June 2020).
6. Doosan Heavy Industries Vying to Join Large Gas Turbine Producers. Available online: <https://www.powereng.com/2019/09/20/doosan-heavy-industries-vying-to-join-large-gas-turbine-producers/> (accessed on 2 June 2020).
7. McBride, B.J.; Zehe, M.J.; Gordon, S. *NASA Glenn Coefficients for Calculating Thermodynamic Properties of Individual Species*; NASA/TP—2002-211556; National Aeronautics and Space Administration: Washington, DC, USA, 2002.

8. Reid, R.C.; Prausnitz, J.M.; Poling, B.E. *The Properties of Gases & Liquids*, 4th ed.; McGraw-Hill: New York, NY, USA, 1988.
9. Atherton, D.P.; Borne, P. *Concise Encyclopedia of Modelling and Simulation*, 1st ed.; Pergamon: Oxford, UK, 1991.
10. Luyben, W.L. *Process Modeling, Simulation and Control for Chemical Engineers*, 2nd ed.; McGraw-Hill: New York, NY, USA, 1989.
11. Mattingly, J.D. *Elements of Gas Turbine Propulsion*; McGraw-Hill: New York, NY, USA, 1996.
12. Brighenti, A.; Bernocchi, A.; Martini, F.; Eierle, C.N.; Stockmann, R. *Simulating Snøhvit Compressors: Part One*; LNG industry, Palladian Publications: Farnham, Surrey, UK, 2007; pp. 47–52.
13. Brighenti, A.; Bernocchi, A.; Martini, F.; Eierle, C.N.; Stockmann, R. *Simulating Snøhvit Compressors: Part Two*; LNG industry, Palladian Publications: Farnham, Surrey, UK, 2008; pp. 89–94.
14. Brighenti, A.; Panikulam, J.V.; Bondi, S.; Fioravanti, L.; Amidei, S.; Gennari, G. Simulator of the Orogen™ system for Waste Heat Recovery from Gas Turbines. In Proceedings of the 32nd CAE Conference, Parma, Italy, 17–18 October 2016.
15. Schobeiri, M.T. *Gas Turbine Design, Components and System Design Integration*; Springer: Berlin, Germany, 2017.
16. Alobaid, F.; Mertens, N.; Starkloff, R.; Lanz, T.; Heinze, C.; Epple, B. Progress in dynamic simulation of thermal power plants. *Prog. Energy Combust. Sci.* **2017**, *59*, 79–162. [[CrossRef](#)]